Development of a Model for Predicting Transient Hydrogen Venting in 55-Gallon Drums - 9416

Jason W. Apperson (ES-SE), James S. Clemmons (EWMO-DO),
Michael D. Garcia (ES-SE), Michael J. Romero (EWMO-TRU),
John C. Sur (ES-DE), Duan Z. Zhang (T-3)

Los Alamos National Laboratory
P.O. Box 1663, Los Alamos, New Mexico, 87545, USA

ABSTRACT
Remote drum venting was performed on a population of unvented high activity drums (HAD) in the range of 63 to 435 plutonium equivalent Curies (PEC). These 55-gallon Transuranic (TRU) drums will eventually be shipped to the Waste Isolation Pilot Plant (WIPP). As a part of this process, the development of a calculational model was required to predict the transient hydrogen concentration response of the head space and polyethylene liner (if present) within the 55-gallon drum. The drum and liner were vented using a Remote Drum Venting System (RDVS) that provided a vent sampling path for measuring flammable hydrogen vapor concentrations and allow hydrogen to diffuse below lower flammability limit (LFL) concentrations. One key application of the model was to determine the transient behavior of hydrogen in the head space, within the liner, and the sensitivity to the number of holes made in the liner or number of filters. First-order differential mass transport equations were solved using Laplace transformations and numerically to verify the results. The Mathematica 6.0 computing tool was also used as a validation tool and for examining larger than two chamber systems. Results will be shown for a variety of configurations, including 85-gallon and 110-gallon overpack drums. The model was also validated against hydrogen vapor concentration assay measurements.

INTRODUCTION
This study initially focused on eleven high activity 55-gallon drums that varied from 65 to 435 PEC. Other than measurements of the PEC content of each drum, limited information was available on the internal packaging configuration of the waste within each of the eleven drums. That is, it was not known, a priori, if the waste was bare waste within the drum, waste contained in thin polyethylene bags, waste within a thick high-density polyester liner, within smaller drums, or some combination. Therefore, the analysis dictated worst-case and conservative bounding calculations for a variety of waste configurations within the 55-gallon drum, including drum overpack configurations. It was assumed conservatively that a 100% hydrogen concentration existed within any sealed “package” such the polyethylene liner within the 55-gallon drum.

The primary objective of these analyses was to determine the transient behavior for hydrogen in the head space to reach a peak value and the corresponding time for the hydrogen in the head space and inner container to reach steady-state equilibrium. Documented Safety Analysis (DSA) requirements considered the drum “vented” when hydrogen concentration levels were less than 25% of the LFL for hydrogen. A secondary objective was to determine the maximum difference in hydrogen concentration between the head space and inner container after attaining the hydrogen peak value in the vapor space.

Operational Summary
Three configurations of drums are to be vented with the Remote Drum Venting System (RDVS). It should be emphasized that these are the processing configurations. These are:

(1) 55-gallon drum

(2) 55-gallon drum inside a 85 gallon overpack
(3) 55-gallon drum inside a 85 gallon overpack, inside a 110 gallon overpack

The overpack configurations are to be vented using a Remote Drum Venting System (RDVS) to vent unvented drums and provide a vapor sampling path for determining flammable vapor concentrations within the drum head space. The 110-gallon unvented overpack is penetrated once. Following the penetration the 110-gallon overpack vapor space is purged with nitrogen and hydrogen is reduced to less than 4% hydrogen by volume. After purging the 110-gallon drum, the lid is removed and the purging process is performed on the 85-gallon drum.

The process on 55-gallon drums is different than the overpacks. No nitrogen purging is performed on the 55-gallon drums. Also, some undetermined number of 55-gallon drums were assumed to have a 48-gallon polyethylene liner within the drum. Carbon diffusion filters were installed on the drum lid to decrease the head space to 25% of the LFL of hydrogen which is 4%. Filters were be installed with sufficient number of filter vents to bound the hydrogen generation rate for the PEC content within the drum. The maximum number of filters is limited by the drum lid area, however, the maximum number installed were expected to be easily accommodated on the drum lid.

After the appropriate number of filters are installed, the 55-gallon drum is prepared for transportation out of the drum venting containment enclosure. If the 55-gallon drum was in an overpack during drum venting activities, only the outer most overpack lid (with appropriate sized filter) is re-installed. Therefore, the venting configuration would be one of the following:

(1) 55-gallon drum
(2) 55-gallon drum inside a 85 gallon overpack
(3) 55-gallon drum inside a 85 gallon overpack (no lid), inside a 110 gallon overpack

Assumptions

One of the most significant assumptions in these models was to assume that there is no absorption of hydrogen within the drum through the formation of hydrides such as PuH_2. We must make this assumption since we do not have detailed information on the contents of the drum. Given this, we must make a conservative assumption to neglect any absorption of hydrogen within the drum.

Hydrogen is generated when alpha particles from the decay of Pu^{239} or Pu^{238}, as well as other radioactive contaminates, interacts with the hydrogenous materials such as polyethylene or polyvinyl chloride (PVC). Westinghouse Savannah River Site (WSRS) developed a hydrogen generation rate of 0.22 millimoles/(day PEC) [1] and was used in these calculations.

Buoyancy of the hydrogen within the drum or liners was also neglected. Based on experimental results by Vaccaro [2] in 20 gallon drums (52 cm height by 48 cm diameter), a 7% gradient was measured with the highest concentration at the top of the drum. Based on this, in an equilibrated drum, the measurement of hydrogen concentration at the top of the inside the drum lid will measure the highest concentration inside the drum and the driving concentration difference for diffusion through openings will likely exceed that assumed in the model.

As a conservative initial condition, it is assumed that the hydrogen concentration in the head space of the 55-gallon drum has not equilibrated with the hydrogen concentration in the liner volume and that the hydrogen concentration in the liner is 100%. That is, as an initial condition, it is assumed that the generated hydrogen in the liner volume has not leaked or diffused a significant amount of hydrogen to the head space during storage.

Buoyancy and convection of hydrogen within the drums is neglected. That is, the concentration of hydrogen in air inside the drum liner and inside the drum head space respectively are assumed to be well mixed and the lighter hydrogen gas does not concentrate near the filters or liner holes where diffusion occurs. This is a conservative assumption. Drums are subject to atmospheric "breathing" phenomena subject to diurnal temperature changes. The phenomena can be due to barometric pressure variations and diurnal temperature changes. WSRS, [3], indicate the daily temperature change is observed to dominate and estimate that values equal to and greater than 0.5 moles/day/ mole-fraction. As they state, the prediction of system performance for these issues is difficult.

The diffusion or any leakage through the liner was assumed to be negligible compared to any hole(s) made in it and ignored in the diffusion calculations. The thin (0.01 cm thick low-density polyethylene sheet) waste bag material within the liner is neglected in the calculations due to its low resistance compared to the liner. Pressures in the bags, liner, and head space are the same as external atmospheric pressure. Volume of the liner is taken as a constant neglecting space occupied by drum contents.

Transient Model Technical Approach

The general approach for addressing most drum configurations was to develop a closed-form and fully-coupled differential solution for a two-chamber system. Laplace transformations were used to solve the set of coupled equations. An Excel spreadsheet was used to plot data.

The powerful Mathematica computing tool (Version 6.0), [4], developed by Stephen Wolfram, was also used as a contingency and validation tool to solve fully-coupled differential equations numerically for examining three-chamber and larger chamber systems.

Analytical Transient Mass Conservation Equations

The mass conservation equation for a two-chamber system is the following two equations.
Mass conservation within the liner with subscript 1 is:

$$Generation = \frac{dm_1}{dt} + \dot{m}_{1\,out} \tag{1}$$

Mass conservation within the head space with subscript 2 is:

$$\dot{m}_{1\,out} = \frac{dm_2}{dt} + \dot{m}_{2\,out} \tag{2}$$

Let ρ_1 and ρ_2 be the hydrogen densities inside the liner and inside the head space, A_1 is the opening area of the liner, A_2 is the opening area of the drum, R_1 is the resistance of the mass transfer across the liner, R_2 is the resistance of the mass transfer from inside the drum to outside air, V_1 is the volume with the liner, and V_2 is the head space volume.

$$G = V_1 \frac{d\rho_1}{dt} + \frac{A_1}{R_1}(\rho_1 - \rho_2) \tag{3}$$

$$\frac{A_1}{R_1}(\rho_1 - \rho_2) = V_2 \frac{d\rho_2}{dt} + \frac{A_2}{R_2}(\rho_2 - 0) \tag{4}$$

Expressing in terms of concentrations or mole fractions

$$G_v = \frac{G}{\rho} \tag{5}$$

Where G is the hydrogen generation rate and G_v is the hydrogen volumetric generation rate

$$G_v = V_1 \frac{\partial C_1}{\partial t} + \frac{A_1}{R_1}(C_1 - C_2) \tag{6}$$

Where C_1 is the hydrogen concentration within the drum liner and C_2 is the hydrogen concentration in the drum head space.

$$\frac{A_1}{R_1}(C_1 - C_2) = V_2 \frac{dC_2}{dt} + \frac{A_2}{R_2} C_2 \tag{7}$$

Analytical Steady-State Solutions

Since there is a constant source term G_v / V_1, these equations have a steady state solution. Expressing $k_1 = A_1/(V_1 R_1)$, $k_2 = A_1/(V_2 R_1)$, and $k_3 = A_2/(V_2 R_2)$. This steady state solution can be obtained by setting $dC_1/dt = dC_2/dt = 0$ in Equations (6) and (7). Namely,

$$0 = -k_1(C_1 - C_2) + \frac{G_v}{V_1} \tag{8}$$

$$0 = k_2(C_1 - C_2) - k_3 C_2 \tag{9}$$

The solutions are

$$C_1^s = \frac{(k_2 + k_3)G_v}{k_1 k_3 V_1} \quad and \quad C_2^s = \frac{k_2 G_v}{k_1 k_3 V_1} \tag{10}$$

where the superscript *s* denotes the steady-state concentration. Therefore the difference at steady-state is:

$$\Delta C^s = \frac{(k_2 + k_3)G_v}{k_1 k_3 V_1} - \frac{k_2 G_v}{k_1 k_3 V_1} = \frac{G_v}{k_1 V_1} = \frac{G_v R_1}{A_1} \tag{11}$$

Transient state and Full Solution

Equations (3) and (4) were cast in second-order form to give the following two equations:

$$\frac{\partial^2 C_2}{\partial t^2} + \frac{V_1 \cdot \frac{R_1}{A_1}\left(\frac{A_1}{R_1} + \frac{A_2}{R_2}\right) + V_2}{V_1 V_2 (R_1 / A_1)} \cdot \frac{\partial C_2}{\partial t} + \frac{(A_2 / R_2)}{V_1 V_2 (R_1 / A_1)} \cdot C_2 = \frac{G_v}{V_1 V_2 (R_1 / A_1)} \tag{12}$$

Similarly for C_1

$$\frac{\partial^2 C_1}{\partial t^2} + \frac{V_1 \cdot \frac{R_1}{A_1}\left(\frac{A_1}{R_1} + \frac{A_2}{R_2}\right) + V_2}{V_1 V_2 (R_1 / A_1)} \cdot \frac{\partial C_1}{\partial t} + \frac{(A_2 / R_2)}{V_1 V_2 (R_1 / A_1)} \cdot C_1 = \frac{G_v \frac{R_1}{A_1}\left(\frac{A_1}{R_1} + \frac{A_2}{R_2}\right)}{V_1 V_2 (R_1 / A_1)} \quad (13)$$

Both Equations (12) and (13) are both independent second-order equations and differ by the term on the right hand side of the equality sign. The general expression for both Equations (12) and (13) is given by:

$$\hat{A}\frac{\partial^2 C(t)}{\partial t^2} + \hat{B}\frac{\partial C(t)}{\partial t} + \hat{C}C(t) = \hat{D} \quad (14)$$

Where $\hat{A}, \hat{B}, \hat{C}, \text{and } \hat{D}$ are constants. Since $\hat{A} = 1$ and by Laplace transformation

$$s^2 f(s) - sf(0) - f'(0) + \hat{B}(sf(s) - f(0)) + \hat{C}f(s) = \frac{\hat{D}}{s} \quad (15)$$

$$f(0) = C_i(0) \quad (16)$$

Where $C_i(0)$ are the initial concentrations within the liner and head space. The indicial notation i refer to the initial concentrations within the liner $C_1(0)$ and head space $C_2(0)$. For the liner volume, the first-derivative initial condition is

$$f_1'(0) = -k_1(C_1(0) - C_2(0)) + \frac{G_v}{V_1} \quad (17)$$

For the head space volume, the first-derivative initial condition is:

$$f_2'(0) = k_2\left(C_1(0) - C_2(0)\right) - k_3 C_2(0) \quad (18)$$

Completing Equation (15) *the* $f_1(s)$ *term is*:

$$f_1(s)(s^2 + \hat{B}_2 s + \hat{C}_2) = sC_1(0) + \hat{B}_1 C_1(0) - k_1(C_1(0) - C_2(0)) + G_v / V_1 + \frac{\hat{D}_1}{s} \quad (19)$$

Completing Equation (15) *the* $f_2(s)$ *term is*:

$$f_2(s)(s^2 + \hat{B}_2 s + \hat{C}_2) = sC_1(0) + \hat{B}_2 C_1(0) + k_2\left(C_1(0) - C_2(0)\right) - k_3\hat{C}_2 + \frac{\hat{D}_2}{s} \quad (20)$$

where $\hat{B}_1 = \hat{B}_2 = k_1 + k_2 + k_3$

and $\hat{C}_1 = \hat{C}_2 = k_1 k_3$

Solving for $f_1(s)$ *in* Equation (19) gives

$$f_1(s) = \frac{s^2 C_1(0) + s\left[\hat{B}_1 C_1(0) - k_1(C_1(0) - C_2(0)) + (G_v / V_1)\right] + \hat{D}_1}{s(s^2 + \hat{B}_1 s + \hat{C}_1)} \tag{21}$$

Solving for $f_2(s)$ *in* Equation (20) gives

$$f_2(s) = \frac{s^2 C_1(0) + s\left[\hat{B}_2 C_1(0) + k_1\left(C_1(0) - C_2(0)\right) - k_3 \hat{C}_2\right] + \hat{D}_2}{s(s^2 + \hat{B}_2 s + \hat{C}_2)} \tag{22}$$

The roots of the term $s^2 + \hat{B}_1 s + \hat{C}_1$ and $s^2 + \hat{B}_2 s + \hat{C}_2$ are the same for $f_1(s)$ and $f_2(s)$ and given by

$$s = -p, -q = \frac{-\hat{B} \pm \sqrt{\hat{B}^2 - 4\hat{A}\hat{C}}}{2\hat{A}} \; where \; \hat{A} = 1 \tag{23}$$

Given the general form of $f_i(s)$ is

$$f_i(s) = \frac{s^2 C_i(0) + s\hat{B} C_i(0) + s f_i'(0) + \hat{D}_i}{s(s^2 + \hat{B}_i s + \hat{C}_i)} \tag{24}$$

Assuming a general form for the Laplace transform of Equation (24)

$$f(s) = \frac{\alpha}{s+p} + \frac{\beta}{s+q} + \frac{\kappa}{s} \tag{25}$$

Where the inverse Laplace transform and general solution of Equation (25) is

$$C(t) = \alpha e^{-pt} + \beta e^{-qt} + \kappa \tag{26}$$

The solution of the numerator in Equation (24) is:

$$(s^2 + \hat{B}s + \hat{C}) = (s+p)(s+q) = s^2 + s(p+q) + pq \quad then \quad p + q = \hat{B} \; and \; pq = \hat{C} \tag{27}$$

Combining Equations (24) and (25) and expanding gives:

$$\alpha(s^2 + qs) + \beta(s^2 + ps) + \kappa(s^2 + (p+q)s + pq) = s^2 C_i(0) + s\hat{B}_i C_i(0) + s f_i'(0) + \hat{D}_i \tag{28}$$

Collecting common terms from Equation (28) follows three independent equations to solve for $\alpha, \beta, and \; \kappa$:

Constant terms in Equation (28) : $pq\kappa = \hat{D}_i \; therefore \; \kappa = \frac{\hat{D}_i}{pq}$ (29)

s^2 terms in Equation (28) : $\alpha + \beta + \kappa = C_i(0)$ (30)

s terms in Equation (28) : $q\alpha + p\beta + (p+q)\kappa = \hat{B}_i C_i(0) + f_i'(0)$ (31)

Solving Equations (30) and (31) for α *and* β gives:

$$\alpha = \frac{q}{q-p}(C_i(0) - \kappa) + \frac{f_i'(0)}{q-p} \quad (32)$$

$$\beta = (1 - \frac{q}{q-p})(C_i(0) - \kappa) - \frac{f_i'(0)}{q-p} \quad (33)$$

Substituting $\alpha, \beta,$ *and* κ into Equation (25) gives the final expression for the concentration in the liner and head space as a function of time:

$$C_i(t) = \left[\frac{q}{q-p}(C_i(0) - \frac{\hat{D}_i}{pq}) + \frac{f_i'(0)}{q-p} \right] e^{-pt} + \left\{ (1 - \frac{q}{q-p}) \left[(C_i(0) - \frac{\hat{D}_i}{pq}) \right] - \frac{f_i'(0)}{q-p} \right\} e^{-qt} + \frac{\hat{D}_i}{pq} \quad (34)$$

where p and q are given by Equation (23), $C_i(0)$ are the initial hydrogen concentrations in the liner and head space, $f_i'(0)$ is given by Equations (17) and (18), and $\hat{D}_i$ are given by the constant terms on right hand side of Equations (12) and (13) .

The two chamber model was used extensively in this analysis and applied to variety of drum configurations. Results for an 8 filter and 9 liner hole transient analysis is shown in Figure 1. Initial conditions are a hydrogen concentration of 100% within the liner and 1% in the headspace. The rapid equilibration of the head space is shown in Figure 2 occurring within 0.2 day (4.8 hours) following puncture of the liner.

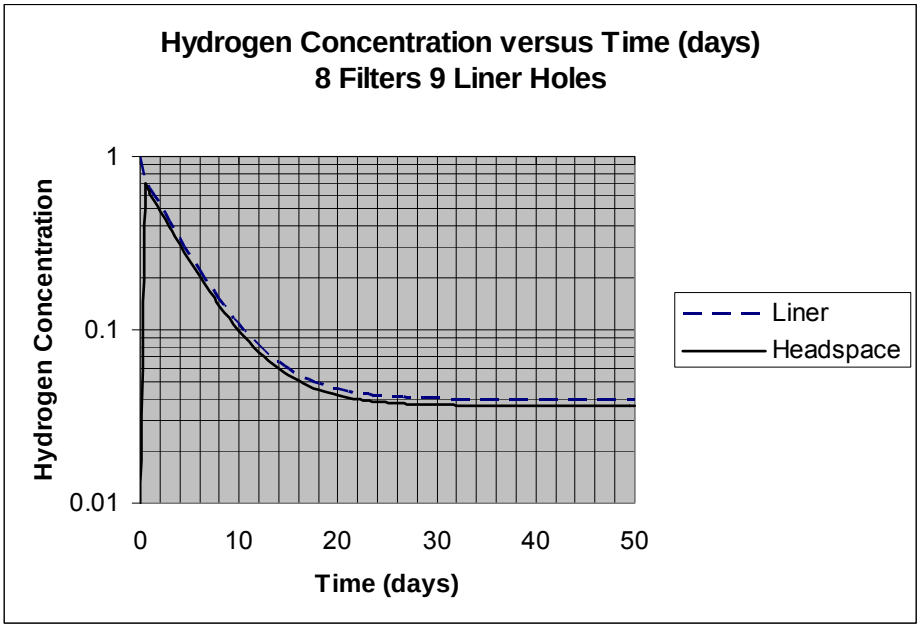

Figure 1: Late-time Response of a 55-gallon drum with 8 Filters and 9 Liner Holes

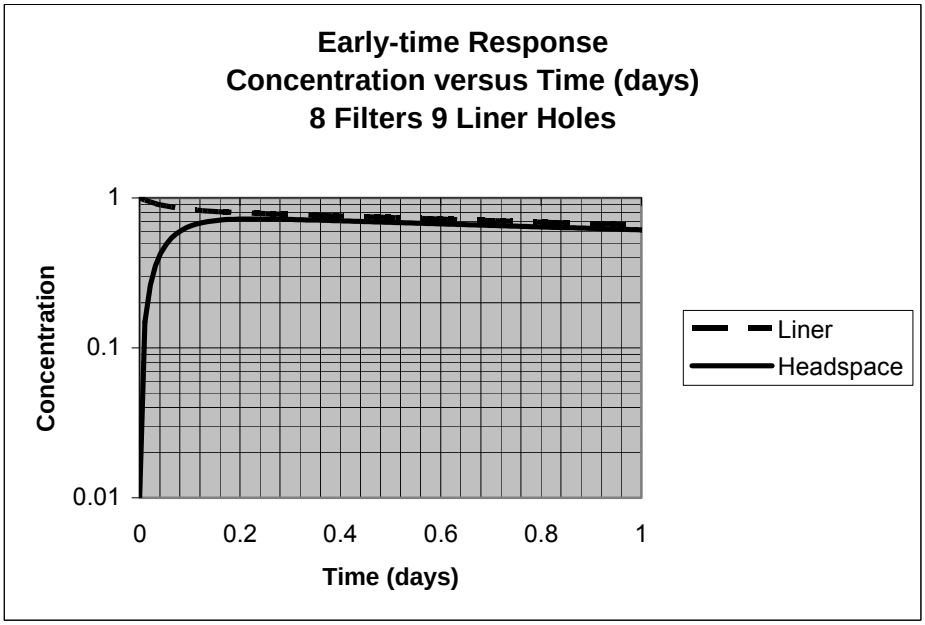

Figure 2: Early-time Response of a 55-gallon drum with 8 Filters and 9 Liner Holes

Three Chamber Model Solved Using Mathematica 6.0

The following set of three coupled first-order differential equations were solved using the Mathematica 6.0 tool using the NDSolve general differential equation numerical solver:

$$\frac{dC_1}{dt} = -k_1(C_1 - C_2) + \frac{G_v}{V_1} \tag{35}$$

$$\frac{dC_2}{dt} = +k_2(C_1 - C_2) - k_3(C_2 - C_3) \quad (36)$$

$$\frac{dC_3}{dt} = +k_4(C_2 - C_3) - k_5(C_3 - C_4) \quad (37)$$

C_1 is the time-dependent concentration within the bag, C_2 is the time-dependent concentration within the rigid liner, C_3 is the time-dependent concentration in the head space, and G_V is the volumetric generation rate within the bag. The constants k_1, k_2, k_3, k_4, and k_5 are the mass transport coefficients between each chamber. A typical computational result is shown in Figure 3 for a single filter on the 55-gallon drum, single hole in the rigid polyethylene liner, and 435 PEC source within the waste bag. The initial hydrogen concentration was assumed to be 1.0 within the bag and 0.1 in the headspace and liner.

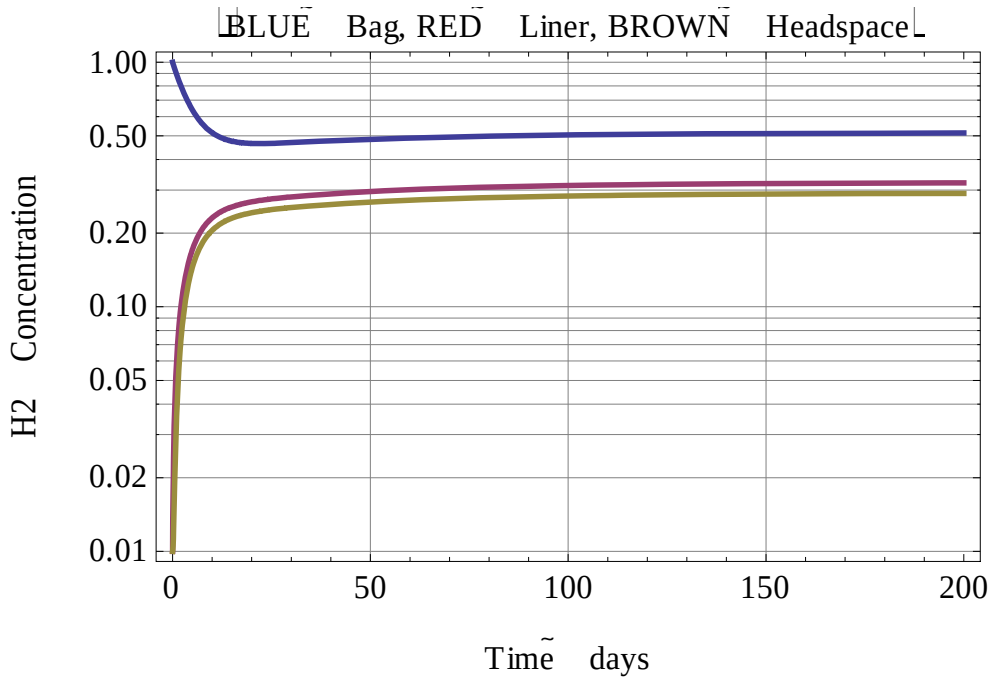

Figure 3: Solving the Coupled Differential Equations Numerically for a Three-chamber System Using Mathematica 6.0.

Preliminary Test Results

During processing of the eleven drums it was determined that each eleven drums had a 30-gallon drum within each of the eleven 55-gallon drum. Visual inspection within the 55-gallon drum also identified a foam filler material located in the headspace apparently to provide physical stability to the 30-gallon drum. There were no liners present in the 55-gallon drum configurations. Initial sampling hydrogen concentration in the headspace ranged from 0.85 to 11.90%, much lower than initial projections. Based on these observations and initial hydrogen concentrations, the two chamber model was used to predict the time for hydrogen to decrease to acceptable levels.

Based on observations that a 30-gallon drum was inserted in the 55-gallon drum and assuming the contents of 30-gallon drum are sealed inside the 55-gallon drum the analysis of this configuration reduced to a single-chamber problem.

Figure 4 shows Drum number S852018 and compares the model with the test data, including an exponential fit to the data. Between 6-days (second sample) and 18-days (third sample) the drum decreased to below 25% of the Lower Flammability Limit (LFL). An unexpected increase (4th sample) to a 1% hydrogen concentration occurred at 20-days. We continue to assess the test data on this drum.

Figure 5 shows Drum S882898 comparison of the model with the test data. In general the model and test data compare well for this case.

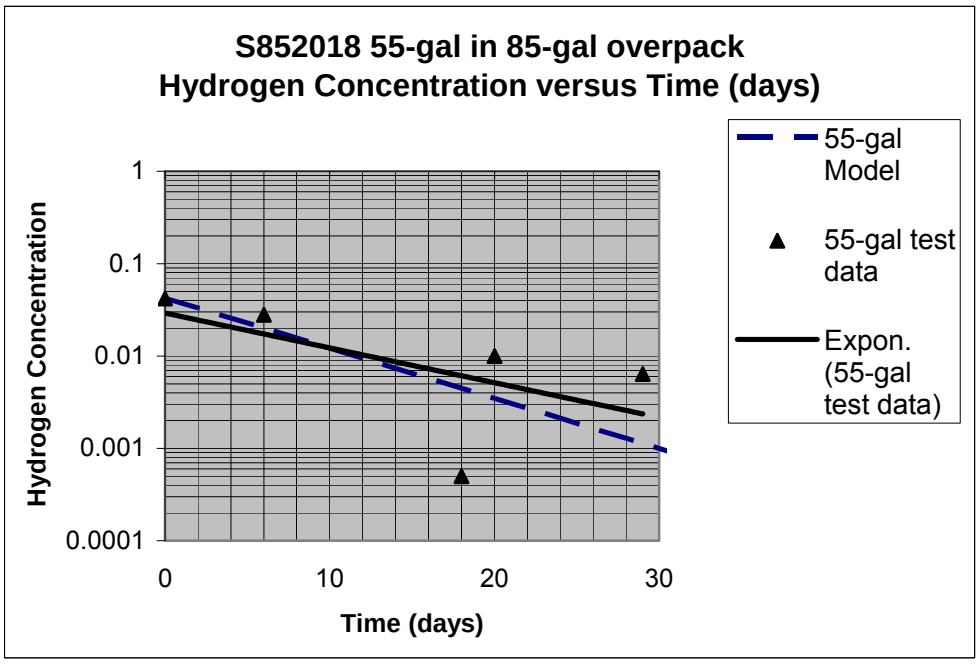

Figure 4: Drum S852018 Comparison of Model with Test Data

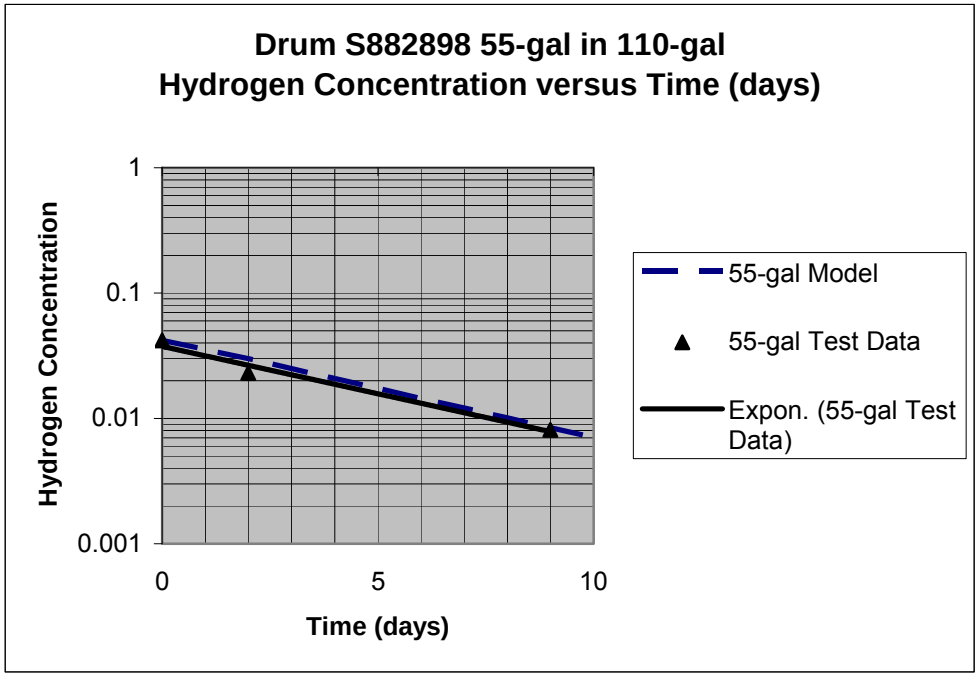

Figure 5: 55-gallon Drum S882898 Comparison of Model with Test Data

Conclusions

While the initial approach to develop a closed-form solution for a two-chamber model was feasible, it is highly recommended that for modeling systems with greater than three chambers that the coupled differential equations are solved numerically with a computational tool like Mathematica.

A highly simplified and conservative model for mass diffusion through the liner hole was applied. The hydrogen mass transport through a hole is actually fairly complex. Penetrations in waste containers were extensively evaluated in the 1980's to address radionuclide transport through the holes as a result of corrosion or cracks in waste containers. It is recommended that more rigorous models for mass diffusion through a hole be developed. We are currently examining the application of more complex and closed-form theoretical models such as those developed in References [5, 6, 7, 8].

Since hydrogen generation rate of 0.22 millimole/(day PEC) induced by radiolysis in the drum is highly conservative, actual equilibration times will be shorter than shown in this calculation. Liner volume and initial concentration inside the liner can be decreased to reduce the time, but their impacts are not as significant as filter capacity.

The steady-state (long-time) concentration in the liner, C_1^S, is highly dependent (directly proportional) on the assumed hydrogen generation rate, G_v, and to the constants (k_1, k_2, and k_3) related to resistance to hydrogen mass transfer through the filter(s) and liner hole(s). The assumed generation rate is highly conservative and will dictate the steady-state concentration in the liner.

The assumed initial concentration in the liner was assumed to be a conservatively large (1.0 or 100%) and the initial concentration in the head space is conservatively assumed to be small (0.01 or 1%). Time to equilibration is not highly sensitive to the initial assumed concentrations within the liner.

For the worst case bounding calculation is the 55-gallon drum within a 110-gallon drum with the lowest PEC of 63.18 and 1 filter. This worst case configuration attains an equilibrium in 60 hours. Therefore, a conservative bound of least 72 hours was estimated to obtain a hydrogen head space concentration measurement (sample) that is representative of the hydrogen concentration within the liner.

The head space and liner equilibrate for an equivalent number of holes as filters. The concentration within the liner is increased by decreasing the number of holes in it.

The concentration in the head space rises rapidly once a single hole is made in it, however, decreasing the number of holes relative to the number of filters does influence the concentration differential between the head space and the liner. The steady-state hydrogen concentration difference between the liner and the head-space is only dependent on the number of holes for a constant G_v and decreases inversely proportional to the number of holes in the liner.

For hydrogen concentration inside the liner to drop below 1% required by current safety analyses for the 11 high-level TRU drums, different filters (other than the NFT-075 [9] filters currently planned to be installed on the 55-gallon drums) with higher diffusivity were recommended. This requirement will apply to all drums being processed. Based on the very conservative assumptions, the goal of a 1% hydrogen concentration was initially predicted to be not feasible within 1 to 2 weeks based on assumed hydrogen generation rate and initial hydrogen concentrations with current filters.

85-gallon or 110-gallon over pack drums were used to contain the 55-gallon drum for contamination control. Due to the high filter capacity of NFT-016SSHP [10], 55-gallon responds similarly as a non overpacked drum with the same number of filters, that is, as though no overpack is present.

References

1. Frequency of a Drum Breach in Solid Waste Management Facility (SWMF), D. Cramer, B. N. Roy, Westinghouse SRS, S-CLC-E-00146, Rev. 0, January 2003.
2. Hydrogen Gas Evolution and Ventilation from Battery Rooms - Experimental Efforts, Frank Vaccaro, Power Battery Co., Inc., Patterson, NJ, 07514.
3. Time to LFL After Venting, Westinghouse SRS, WSRC-STI-2007-00582, Revision 0, R. F. Bradley and S. J. Mentrup, October 2007.
4. *Wolfram* Mathematica 6.0, Wolfram Research Inc., http://www.wolfram.com.
5. Steady-state and Transient Radionuclide Transport Through Penetrations in Nuclear Waste Containers, P. L. Chambré, W, W. L. Lee, C. L. Kim and T. H. Pigford, LBL-21806, UC-70, July 1986.
6. Radionuclide Transport Through Perforations in Nuclear Waste Containers, C. K. Aidun, S. G. Bloom, G. Raines, Material Research Society Symposium, Volume 112, 1988.
7. Radionuclide Mass Transfer Rates From a Pinhole in a Waste Container For An Inventory-Limited and Constant Source, D. M. LeNeveu, Nuclear Technology, Volume 123, August 1998.
8. A Numerical Study of Transient Mass Transport Through a Circular Hole Connecting Two Semi-Infinite Media, D. W. DePaoli and T. C. Scott, Nuclear Technology, Volume 101, January 1993.
9. Product Specification Data Sheet for NucFil 075, January 1, 2006.
10. Product Specification Data Sheet for NucFil®016SSHP, March 12, 2004.